Development of a Physics-Inspired Model for the Characterization of Vapor Injected Compressors

Amjid Khan[1]*, Craig R. Bradshaw[2]

[1,2]Center for Integrated Building Systems, Oklahoma State University,
Stillwater, Oklahoma, US
[1]amjid.khan@okstate.edu, [2]craig.bradshaw@okstate.edu

* Corresponding Author

ABSTRACT

This paper presents a new physics-inspired model to represent vapor-injected compressors. The developed model was inspired from the polytropic nature of compression processes. The resulting model is a pressure ratio-based model using suction, injection, and discharge pressures to predict evaporator mass flow rate, injection mass ratio, compressor power, and discharge temperature. To evaluate the model's predictive capabilities, a dataset containing 4, in-house, combinations of compressors with different refrigerants and 3 datasets collected from the literature were used. The deviation from experimental results for the evaporator mass flow rate, and input compressor power were lower than 5% Mean Absolute Percentage Error (MAPE) in all cases of interpolation, with the exception of few extrapolation cases. The deviation from experimental results for the discharge temperature was lower than 3K Mean Absolute Error (MAE) in all cases.

1. INTRODUCTION

Refrigerant injection is a technique used to enhance the performance and reliability of heat pumps, particularly in challenging environmental conditions. This method involves redirecting a portion of the refrigerant from the condenser outlet back into the compressor at an intermediate stage of the compression process. By injecting vapor, the circulation of refrigerant in the condenser is increased, leading to higher heating capacities. Since a portion of the refrigerant is injected into the compressor at an intermediate pressure, less specific compression work is needed compared to a non-injected compressor (Xu et al. 2011)

Refrigerant injection can be performed in three ways, liquid injection, vapor injection, or two-phase injection. Yang et al., (2015) performed a computational investigation of three techniques to reduce the discharge temperature through two-phase suction, liquid injection, vapor injection, and two-phase injection. All these methods showed very promising results. It was concluded that two-phase/vapor injection outperforms both liquid injection and two-phase suction in both cooling capacity and COP by 11.8% and 4.8% respectively. It means for improving the air source heat pumps performance improvement, vapor injection is one of the most favorable techniques.

A significant amount of vapor injection research concerning scroll and rotary compressors has been dedicated to enhancing the performance of the air source heat pumps. The main two approaches used to implement vapor injection are closed economized system and flash tank system. Ma and Zhao, (2008) conducted an experimental investigation into the vapor injection heat pump cycle, incorporating a flash tank coupled with a scroll compressor. Wang et al. (2009) explored the performance of a 11kW R410A heat pump system employing a two-stage vapor injected scroll compressor through experimental means, thereby establishing fundamental design and operational guidelines for heat pump systems. Concurrently, similar experimental investigations of vapor-injected compressors showed enhanced performance, showing the significance of economization and vapor injection, as evidenced by (Xu et al. 2011, Bertsch and Groll 2008, Yang et al. 2015, Cho et al., 2012, Khan and Bradshaw 2023). Currently, research on vapor injection compressors is either focused on vapor injection compressor design optimization or compressor modeling. However, unlike conventional scroll compressors devoid of injection, conventional efficiency models like the AHRI 10-coefficient model, are inadequate for representing the performance of injection scroll compressors due to the variable parameters associated with injected refrigerants. Even though accurate models are very important for prediction of compressor performance, efficiency, and operational capabilities. Accurate compressor models can improve the performance of overall system by assessing energy consumption under varying conditions accurately. Furthermore,

the unavailability of common modeling approach for vapor injected compressors makes it complicated for its integration in heat pump systems.

Previously, in literature, there have been attempts to develop physics-based models i.e., mechanistic chamber model, which provides deep understanding of the detailed geometrical and thermodynamic phenomena within the compressor capturing compressor performance more accurately (Bradshaw et al. 2016; Orosz et al. 2014; Islam et al. 2021, Tanveer et al. 2022; Tanveer and Bradshaw 2021). These models are generally very detailed and very specific for compressor design purposes, providing high fidelity representation of compressor behavior but at the cost of high computational time. However, at system level, the focus shifts towards the performance prediction and system integration. Consequently, researchers have extensively explored semi-empirical or black box models tailored for vapor injection compressors (Tello-Oquendo et al., 2017, Lumpkin et al., 2019, Winandy et al., 2002, Dardenne et al. 2015).

The black-box model is one of the modelling approaches, which does not rely on specific physical information regarding compression and injection processes within the compressor. Instead, these models typically comprise polynomial equations, where the coefficients are adjusted to match experimental data. Tello-Oquendo et al., (2017b), modified the AHRI polynomial model for compressors with vapor injection by estimating the suction mass flow rate through the existing AHRI polynomial model. They established the ratio of injection mass flow rate to suction mass flow rate via a linear correlation dependent on the ratio of injection to suction pressure. Furthermore, they incorporate a modified version of the AHRI polynomial model, augmented with an additional linear term to consider the injection dew point temperature, to predict power consumption. Additionally, the authors derive the injection pressure based on the energy balance and heat transfer principles associated with the specific vapor injection mechanism utilized in the cycle, such as the economizer or flash tank. Lumpkin et al., (2018b) developed a dimensionless-PI correlation for mapping injection ratio and compressor power consumption. Navarro et al., (2013) developed black-box model which only captured the injection mass flow rate. The correlation for injection mass flow rate was a first-order polynomial function of evaporating mass flow rate ($\dot{m}_e$) and injection to evaporator pressure ratio $\left(P_{inj}/P_e\right)$. Khan and Bradshaw (2024b) proposed vapor injected mapping characterization to predict compressor power, evaporator mass flow rate, injection mass flow rate as output parameters. All these output parameters are the function of evaporator pressure (P_e), injection pressure (P_{inj}), and condensing pressure (P_{cond}). All these black box models have either 10 or more coefficients, require 10 or more data points to train the model for performance prediction.

The semi-empirical models are derived from fundamental work equations of the vapor compression process and employ less experimental data to predict the compressor performance with higher accuracy. Dardenne et al. incorporated modifications to Winandy and Lebrun model to accommodate the complexities associated with vapor injection (Winandy et al., 2002, Dardenne et al. 2015). These enhancements necessitated the incorporation of added parameters to address the influence of vapor injection on key compressor performance outputs, encompassing suction mass flow rate, injection mass flow rate, input power consumption, and discharge temperature. The resultant model integrates ten parameters, each possessing tangible physical significance, and practiced validation against a comprehensive dataset comprising 63 steady-state experimental measurements. Sun et al., (2018) developed correlations for compressor output parameters to enable accurate and computationally efficient predictions. These correlations require empirical parameters, with the suction mass flow rate model needing five, injection mass flow rate model needing eight, compressor input power model needing twelve, and discharge enthalpy model needing one. Tello-Oquendo et al., (2019) developed semi-empirical model to account for the main sources of losses in the compression process. This model had 10 empirical parameters to predict compressor and volumetric efficiencies, discharge temperature, compressor power, and mass flow rate through suction and injection ports. This model was validated with non-injected scroll compressor tested with R290 and a scroll compressor with vapor injection tested with R207C. Similar studies were carried out developing semi-empirical compressor models, which studied the added complexities of vapor injection in the compressor in detail by (Qiao et al., 2015, Dechesne et al. 2019)

In this paper, a physics-inspired modeling methodology is proposed for predicting the performance of vapor injected compressors. In particular, the study will focus on the development of model for each compressor output parameter including compressor power consumption, discharge temperature, and evaporator mass flow rate. The model will also be capable of predicting the performance for fixed and variable speed compressors with or without vapor injection. In literature, most models for variable speed compressor performance prediction require 10 or more experimental data

points to tune the model's coefficients. In this study, a model is developed which does not require extensive experimental testing and also requires computational time similar to black-box models.

2. EXPERIMENTAL DATA COLLECTION AND COMPILATION

Experimental data is compiled from 7 vapor injected compressors of 2 technology types (rotary and scroll), using 3 refrigerants for a total of 216 steady state data points to be used for model training and evaluation. The majority of this data is collected by the authors (116 data points), with supplemental data collected from the literature.

2.1 Experimental Data Collection – In House Data

For the in-house data collection, the hot-gas bypass load stand has been used for collection of data on two scroll and rotary compressors with refrigerants, R410A and R454B. The load stand is capable of testing both traditional and economized compressors at saturated suction temperature as low as -34.44 ℃ (-30 ℉) and saturated discharge temperature as high as 60 ℃ (140 ℉). The design capacity for the load stand is 1-5 tons (3.52-17.5 kW) compressor capacity. Complete operational details and uncertainty of the load stand is presented in (Khan and Bradshaw 2024a). Performance data for two compressor technologies, scroll and rotary, are collected with two working fluids, R410A and R454B with a total of 116 data points. The compressors are commercially available hermetic compressors originally designed for operation with R410A. The scroll compressor has a rated capacity of 5 tons and the rotary 3.25 tons. The complete test matrix was developed based on one factor at a time design of experiments method. The final test matrix collected data at evaporating temperatures ranging from -34.44 ℃ to 10 ℃ (-30 ℉ to 50 ℉), condensing temperatures ranging from 23.8 ℃ to 54.44 ℃ (75 ℉ to 130 ℉), superheat from 2.8 ℃ to 16.7 ℃ (5 ℉ to 30 ℉), and speeds from 1800 rpm to 6000 rpm.

Supplemental experimental data was also collected from literature including data for a scroll compressor from Dardenne et al. (2015), Lumpkin et al., (2018), and Tello-Oquendo et al. (2017b), tested with R407C as shown in Table 1. A summary of the data sets for the analysis of the models with compressor type, refrigerant, number of data points, and collection standard is shown in Table 1. The full data set is then divided into two subsets for each model performance evaluation, training and testing data set.

Table 1: Compiled experimental data sets

Compressor Type	Capacity	Refrigerant	Data Points	Collection Standard
Rotary (In-House)	3.25 tons	R410A	29	ASHRAE 23.1
Rotary (In-House)	3.25 tons	R454B	29	ASHRAE 23.1
Scroll (In-House)	05 tons	R410A	29	ASHRAE 23.1
Scroll (In-House)	05 tons	R454B	29	ASHRAE 23.1
Scroll (Tello-Oqu. et al., 2017b)	4.74 tons	R407C	16	ISO
Scroll (Lumpkin et al., 2018b)	-	R407C	21	ASHRAE 23.1
Scroll (Dardenne et al. 2015)	03 tons	R407C	63	ASHRAE 23.1

2.2 Training and Testing Data Sets

Each full data set collected is somewhat unique in its operating envelope and parameters varied, therefore the number of splits (training and testing data sets) is unique. For example, the data from Tello-Oquendo et al., (2017b) had total of 16 datapoints for scroll compressor and did not include variable speed and variable superheat, while data from Dardenne et al., (2015b) had total of 63 datapoints for scroll compressor and did not include variable superheat. Hence, there are only two splits shown in Figure 1, which represent the training set and testing set for both cases of interpolation and extrapolation. For interpolation scenario, training data set are the exterior envelope points with respect to overall envelope as shown in Figure 1 (left), within the complete data set. In addition to the data points at the exterior envelope, two variable speed points and two variable superheat points are added into the training data set. The reason for these additional points is to ensure a model has seen points at different speeds and superheats before exposing it to the variable speed or variable superheat testing data points. These additional points are selected such that one point is above nominal speed and superheat, while the other point is at conditions below nominal speed and superheat. For instance, the rotary compressor R410A in-house data set, the compressor was tested at 30, 50, 70, 80, 90, and 100 Hz. The nominal speed was 80 Hz, the points included in the training data sets were 30 Hz and 100 Hz.

In case of extrapolation, central envelope points shown in Figure 1 (right), are taken as training data points while the exterior envelope points are taken as testing data points.

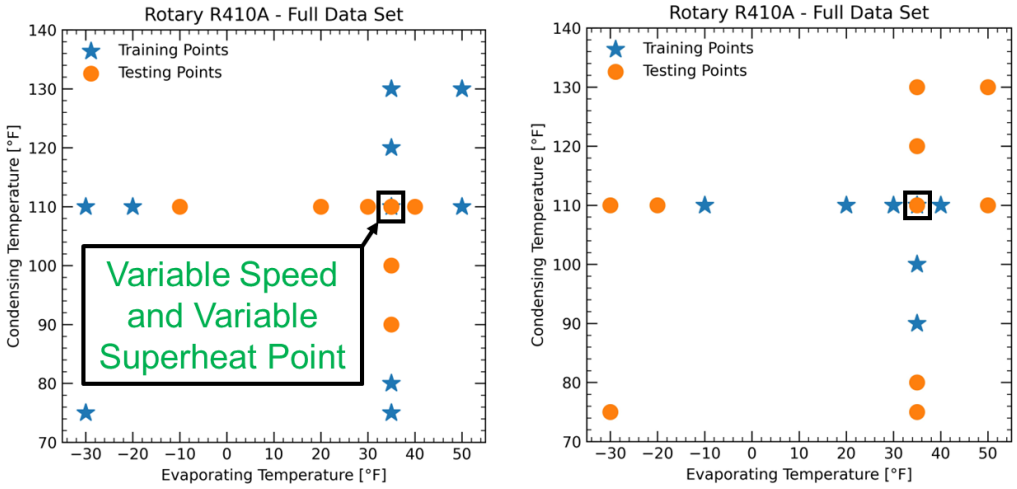

Figure 1: Points selection for interpolation (left) and extrapolation (right)

3. DEVELOPMENT OF PHYSICS INSPIRED MODEL

The proposed compressor performance model consists of 3 sub-models: mass flow rate models, compressor power consumption, and discharge temperature. The flow rate model is on the concept of volumetric efficiency and can be used to evaluate volumetric flow rate and then evaporator mass flow rate. The input power model and discharge temperature are inspired from polytropic process with the additional terms for injection parameters and variable speed. The modeling approach in this work requires several inputs describing the operational conditions of the compressor, including:

- Evaporating or compressor suction pressure, P_{evap}
- Injection pressure, P_{inj}
- Condensing or compressor discharge pressure, P_{dis}
- Nominal discharge temperature, $P_{dis,nom}$
- Compressor rotational speed, ω
- Compressor suction temperature, T_{suc}

3.1 Development of Mass Flow Rate Model

The approach proposed to develop model for mass flow rate is based on drawing mass flow rate to compressor suction and injection port. Compression chamber is a fixed volume based on the compression chamber design represented as displacement volume, but the mass flow rate varies based on compressor speed. During compressor operation, the theoretical volumetric flow rate is the product of displacement volume and compressor rotational speed.

$$\dot{V}_{th} = V_{dis} * \omega \tag{1}$$

During the refrigerant drawing process, theoretically the compression chamber would fill with refrigerant but practically heat transfer, pressure drops, and leakage may prevent the compressor from operating at its theoretical flow rate. To measure this deviation of the actual volumetric flow rate from theoretical can be characterized by volumetric efficiency. Volumetric efficiency, η_v, is the actual volumetric flow rate of refrigerant drawn to compressor to the theoretical volume of the chamber,

$$\eta_v = {\dot{V}_{act}}/{\dot{V}_{th}}, \tag{2}$$

combining equation 1 and 2, effective displacement of the compressor can be written as,

$$\frac{\dot{V}_{act}}{\omega} = \eta_v * V_{dis}, \tag{3}$$

since the volumetric efficiency is unlikely to remain constant, it will be dependent on the operating condition of the compressor, a generic equation is proposed to account for this variation,

$$\frac{\dot{V}_{act}}{\omega} = a_0 + a_1\left(\frac{P_{dis}}{P_{evap}}\right), \tag{4}$$

where a_0 and a_1 are empirical parameters determined from the experimental data.

To determine the evaporator volumetric flow rate for vapor injected compressors, equation 4 is modified to include extra empirical parameter for compressor speed variation and injection pressure to suction pressure ratio to account for injection condition. The proposed correlation for evaporator volumetric flow rate,

$$\dot{V}_{evap} = a_0 + a_1 * \omega + a_2 * \left(\frac{P_{dis}}{P_{evap}}\right)^{a_3} + a_4 * \left(\frac{P_{inj}}{P_{evap}}\right)^{a_3}, \quad (5)$$

where coefficients a_0 to a_4 are empirical parameters and can be determined from experimental data. Exponent a_3 is added into equation to better fit the experimental data. Now evaporator mass flow rate can be found by density equation shown below,

$$\dot{m}_{evap} = \rho_{suc} * \dot{V}_{evap}, \quad (6)$$

To calculate injection mass flow rate, injection mass ratio model from Tello-Oquendo et al. (2017b), is modified to incorporate compressor rotational speed to account for variable speed compressors,

$$\frac{\dot{m}_{inj}}{\dot{m}_{evap}} = b_0 + b_1 * \left(\frac{P_{inj}}{P_{evap}}\right) + b_2 * \left(\frac{\omega_{act}}{\omega_{nom}}\right), \quad (7)$$

in equation 7, the actual compressor speed is normalized by nominal compressor speed. Nominal condition means design condition speed for a specific compressor. The actual compressor speed is also normalized by the minimum and maximum compressor speed in the data set for better understanding, upon evaluation, it also predicted almost similar results for injection mass flow rate. To calculate the total mass flow rate, $\dot{m}_{cond}$, at the compressor discharge, mass balance is applied on evaporator and injection mass flow rate,

$$\dot{m}_{cond} = \dot{m}_{evap} + \dot{m}_{inj}, \quad (8)$$

3.2 Development of Compressor Power Model

The polytropic compression process for reversible rate of work is given by,

$$\dot{W}_{comp} = \frac{n}{n-1} * \dot{m}_s * p_s * v_s \left[\left(\frac{P_{dis}}{P_{evap}}\right)^{\frac{(n-1)}{n}} - 1\right], \quad (9)$$

where n is the polytropic index of the process, which characterizes the type of the thermodynamic process that an ideal gas is undergoing:

- $n = 0$: an isobaric process
- $n = 1$: an isothermal compression process
- $n = \gamma = c_p/c_v$: an isentropic process
- $n = \infty$: an isochoric process

Equation 9 shows the minimum power to compress gas following a polytropic process, it can be generalized to make a dimensionless power correlation. Since equation 9, represents ideal compression work, which in practical applications is higher because of mechanical friction, motor inefficiencies, and other thermodynamic losses. Also, many gases do not behave ideally under high pressure conditions, that's why equation 9 should be generalized to fit it to actual compression process.

$$\dot{W}_{comp} = c_1 \left[\left(\frac{P_{dis}}{P_{evap}}\right)^{c_2} - 1\right], \quad (10)$$

To further modify equation 10 for vapor injection compressors, compressor speed, coefficient for biases, injection pressure to suction pressure ratio, and normalized discharge pressure ratio is added. Compressor speed term is added to account for variable speed compressors. c_0 is added an additional coefficient to account for biases. Injection pressure to suction pressure ratio is added as a representative of injection conditions. In practical applications, compressor power consumption is more effected by the variation of discharge pressure, therefore normalized discharge pressure term is included,

$$\dot{W}_{comp} = c_0 + c_1 * \omega + c_2 * \left(\frac{P_{dis}}{P_{suc}}\right)^{c_3} + c_4 * \left(\frac{P_{inj}}{P_{suc}}\right)^{c_3} + c_5 * \left(\frac{P_{dis}}{P_{dis,nom}}\right)^{c_3}, \quad (11)$$

where c_0 to c_5 are the empirical parameters to be fitted based on experimental data. c_3 exponent is included to account for polytropic index to simulate actual polytropic compression process. In normalized discharge pressure term, $P_{dis,nom}$ stands for design discharge pressure to normalize the discharge pressure for the analysis. If in case, design discharge pressure is unknown or ambiguous, then in that case any pressure from minimum to maximum in data set can be used as $P_{dis,nom}$. It has been evaluated and the results were almost similar for taking any discharge pressure for normalizing.

3.3 Development of Compressor Discharge Temperature

The discharge temperature correlation is a relation between temperatures and pressures for polytropic compression process can be written as,

$$\frac{T_{dis}}{T_{suc}} = \left(\frac{P_{dis}}{P_{evap}}\right)^{n-1/n}, \tag{12}$$

To generalize this equation to fit to experimental data, it can be written as,

$$T_{dis} = T_{suc} * \left(\frac{P_{dis}}{P_{evap}}\right)^{d_1}, \tag{13}$$

where d_1 is empirical parameter to fit to experimental data.

To further modify equation 13 for vapor injection compressors, compressor speed, coefficient for biases, and injection pressure to suction pressure ratio is added. Compressor speed term is added to account for variable speed compressors. d_0 is added an additional coefficient to account for biases. Injection pressure to suction pressure ratio is added as a representative of injection conditions.

$$T_{dis} = d_0 + d_1 * \omega + T_{suc} * \left[d_2 * \left(\frac{P_{dis}}{P_{evap}}\right)^{d_3} + d_4 * \left(\frac{P_{inj}}{P_{evap}}\right)^{d_3}\right], \tag{14}$$

where d_0 to d_4 are the empirical parameters to be fitted based on experimental data. d_3 exponent is included to account for polytropic index to simulate actual polytropic compression process.

3.4 Error Metric to Evaluate Model Performance

The proposed model is trained then evaluated for its ability to predict compressor power, evaporator mass flow rate and discharge temperature. The model is initially trained with full data and then trained with 10 data points from each dataset for multiple compressor technologies and different refrigerants. Following the training phase, the performance of the trained model is evaluated by comparing its predictions against the corresponding test data obtained from experiments as described in Sections 2. The evaluation of model performance is quantified using the Mean Absolute Percentage Error (MAPE), which serves as a metric to measure the accuracy and effectiveness of the models in predicting the desired outcomes,

$$MAPE = \frac{100}{n}\sum_{i=1}^{n}\left|\frac{Y_{true,i} - Y_{predict,i}}{Y_{true,i}}\right|, \tag{15}$$

where n is the total number of data points in the data set, i is each data point, $Y_{true,i}$ and $Y_{predict,i}$ are the model measured data value and model predicted data value for any performance parameter. The MAPE is calculated for both compressor power and evaporator mass flow rate.

The Mean Absolute Error (MAE) is a metric used to evaluate accuracy. It measures the average absolute difference between the actual and predicted values. In this paper, MAE is used to calculate the error difference of temperature in Kelvin. The formula for calculating the Mean Absolute Error is:

$$MAE = \frac{1}{n}\sum_{i=1}^{n}|y_i - \hat{y}_i|, \tag{16}$$

Where n stands for number of samples, y_i stands for the actual value of target variable, $\hat{y}_i$ stands for the predicted value of target variable. MAE is used to calculate the absolute differences between the actual and predicted values across all samples in the dataset specifically used for temperature.

4. RESULTS AND DISCUSSION

In the current study, a physics inspired model was developed and implemented in python. Thermodynamic properties of the fluid i.e., density, were evaluated in CoolProp. The parameters of the models are determined through the minimization of respective objective functions, which encapsulate the sum of squared errors between observed and predicted values, for variables such as compressor power, evaporator mass flow rate and discharge temperature. This minimization process is executed utilizing a nonlinear curve fitting algorithm provided by the SciPy library, facilitating the optimization of model parameters to best fit the experimental data.

The parameters of the compressor power and discharge temperature model are obtained by the curve fitting algorithm. As shown in Figure 2, parity plot is drawn between experimentally measured and model predicted values for both compressor power and discharge temperature. As depicted from the Figure, the MAPE values predicted by the proposed model are less than 2% showing model's capability. It can be clearly seen, almost all of the points are along a straight line, which highlights the reliability of the proposed model in prediction of compressor power and compressor discharge temperature. It should be noted that compressor power showed significant dependency on the discharge pressure in performance evaluation. The inclusion of compressor discharge pressure significantly reduced the MAPE values for the model.

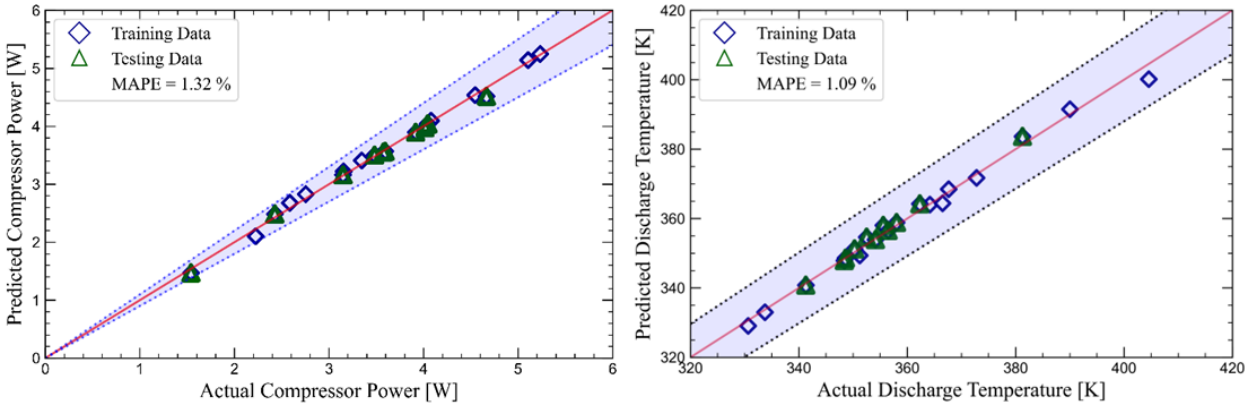

Figure 2: Physics Inspired Model Results for Compressor Power (left) and Discharge Temperature (right)

MAPE for power model predicted parameter is summarized in Table 3. The MAPE values are evaluated in 3 cases of training the model: full data interpolation, 10 data points interpolation, and 10 data points extrapolation. It can be seen that all the data sets when trained with full data showed less than 2% MAPE for compressor power with the exception of scroll compressor R454B data. The compressor power model is then trained with 10 data points for each data set in case of interpolation shown in Figure 1, the MAPE for interpolation with 10 data points was less than 2% except for the case of R454B data with scroll and rotary compressor. Extrapolation analysis is also carried out for all the data sets training the model with 10 exterior envelope points as shown in Figure 1. The results for extrapolation in table 3 are less than 3% MAPE for most of the cases except R454B data for scroll and rotary compressors.

Table 2: Summary of Physics inspired model for Compressor Power.

Datasets	MAPE (%) Interpolation	MAPE (%) Interpolation	MAPE (%) Extrapolation
Training Data	Full Dataset	10 Data Points	10 Data Points
Rotary R410A	1.322	1.381	1.866
Rotary R454B	1.415	2.27	6.146
Scroll R410A	0.7344	1.170	2.548
Scroll R454B	2.83	3.84	6.641
Tello-Oquendo	0.515	0.625	0.847
Lumpkin	1.609	1.552	2.289
Dardenne	0.433	0.875	1.293

The Mean Absolute Error (MAE) for the discharge temperature model's predicted results are summarized in Table 3. Three distinct scenarios are considered for model training: full data interpolation, interpolation with 10 data points, and extrapolation with 10 data points. Notably, when trained with complete datasets, all models exhibit MAE values for discharge temperature below 2 K, except for the Dardenne dataset. Subsequently, the discharge temperature model is trained with 10 data points for each dataset in the interpolation scenario, yielding MAE values below 2 K, with the exception of the Dardenne dataset. Moreover, extrapolation analysis employing 10 exterior envelope points reveals MAE values below 3 K for all datasets, as depicted in Table 3.

Table 3: Summary of Physics Inspired model results for compressor discharge temperature

Datasets	MAE (K) Interpolation	MAE (K) Interpolation	MAE (K) Extrapolation
Training Data	Full Dataset	10 Data Points	10 Data Points
Rotary R410A	1.093	1.193	1.59
Rotary R454B	1.194	1.241	1.055
Scroll R410A	1.193	1.292	1.981
Scroll R454B	1.579	1.821	2.04
Lumpkin	1.635	1.988	2
Dardenne	2.03	2.654	2.055

Figure 3 illustrates a parity plot comparing experimentally measured and model-predicted values for evaporator mass flow rate. The proposed model demonstrates MAPE values below 2%, indicating its robustness. Notably, the majority of data points align closely with a straight line, affirming the reliability of the model in predicting evaporator mass flow rate. It is noteworthy that evaporator mass flow rate exhibits considerable sensitivity to the injection to suction pressure ratio during performance assessment. Additionally, the injection mass flow rate is contingent upon the evaporator mass flow rate, as evidenced by equation 7. Therefore, improved accuracy in predicting the evaporator mass flow rate leads to enhanced performance in predicting the injection-to-evaporator mass ratio and, consequently, the injection mass flow rate.

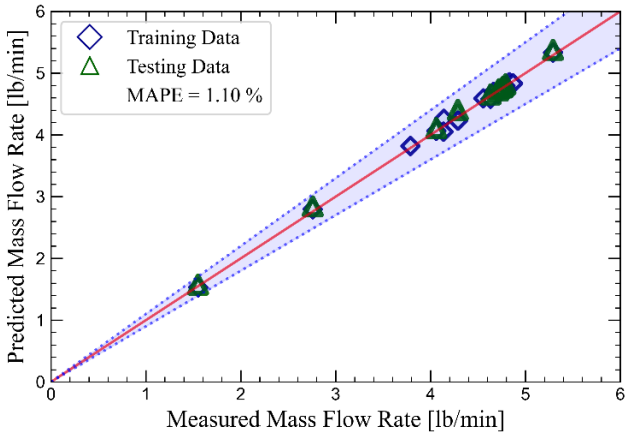

Figure 3: Physics inspired model results for evaporator mass flow rate

Table 4 presents the Mean Absolute Percentage Error (MAPE) for the evaporator mass flow rate model's predictions. Three training scenarios are investigated: full data interpolation, interpolation with 10 data points, and extrapolation with 10 data points. Remarkably, under complete data set training, all data sets demonstrate MAPE values for evaporator mass flow rate below 2%. Subsequently, the evaporator model is trained using 10 data points for each dataset in the interpolation scenario, resulting in MAPE values below 2%. Additionally, extrapolation analysis utilizing 10 exterior envelope points as the training dataset reveals MAPE values below 3% for all datasets, except for scroll compressor R410A and R454B data, as described in Table 4.

5. CONCLUSION

In this study a physics inspired model is presented for vapor injected compressors. The model was developed for the main output parameters of vapor injected compressors i.e., compressor input power, discharge temperature, evaporator mass flow rate, and injection mass flow rate. The models have been applied to seven data sets out of which 4 were in-house data for rotary and scroll compressors with refrigerants R410A and R454B and 3 data sets were collected from the literature. The data contained ranges of pressure ratios, suction superheat, and variable speed.

The parity plots demonstrate the model efficacy in predicting compressor power and discharge temperature, with MAPE values consistently below 2%. Notably, the inclusion of compressor discharge pressure in the evaluation for compressor power prediction significantly improved model performance.

Table 4: Summary of Physics inspired model for evaporator mass flow rate.

Datasets	MAPE (%) Interpolation	MAPE (%) Interpolation	MAPE (%) Extrapolation
Training Data	Full Dataset	10 Data Points	10 Data Points
Rotary R410A	1.104	1.149	1.745
Rotary R454B	0.815	1.134	2.269
Scroll R410A	1.438	1.610	4.485
Scroll R454B	1.089	1.980	4.407
Tello-Oquendo	0.358	0.508	1.017
Lumpkin	0.452	0.622	0.544
Dardenne	1.305	1.455	2.761

The robustness of the proposed model in predicting evaporator mass flow rate, with MAPE values consistently below 2% and a high degree of alignment between experimental and predicted values is shown. Furthermore, the summarized results provide additional insight into the model performance across various training scenarios i.e., interpolation and extrapolation, reaffirming its reliability in predicting evaporator mass flow rate. Overall, the findings suggest that the developed physics-inspired model holds promise for accurate and reliable predictions of key parameters in vapor injected compressors, thus contributing to advancements in system design and optimization.

NOMENCLATURE

$\dot{m}_{inj}$	Mass flow rate through the injection line	[kg/s]
$\dot{m}_{evap}$	Mass flow rate through evaporator	[kg/s]
p_{cond}	Condensing pressure	[kPa]
p_{int}	Injection pressure	[kPa]
p_{evap}	Evaporating pressure	[kPa]
p_{dis}	Discharge pressure	[kPa]
T_{dis}	Discharge temperature	[°C]
T_{suc}	Suction temperature	[°C]
$\dot{W}_{comp}$	Compressor power	[kW]

Abbreviations

AHRI	Air-Conditioning, Heating, and Refrigeration Institute
MAPE	Mean Absolute Percentage Error
MAE	Mean Absolute Error

Greek Symbols

ω	Compressor speed	[rpm]

REFERENCES

Bertsch, Stefan S., and Eckhard A. Groll. 2008. "Two-Stage Air-Source Heat Pump for Residential Heating and Cooling Applications in Northern U.S. Climates." International Journal of Refrigeration 31 (7): 1282–92. https://doi.org/10.1016/J.IJREFRIG.2008.01.006.

Cho, Il Yong, Suk Bin Ko, and Yongchan Kim. 2012. "Optimization of Injection Holes in Symmetric and Asymmetric Scroll Compressors with Vapor Injection." International Journal of Refrigeration 35 (4): 850–60. https://doi.org/10.1016/j.ijrefrig.2012.01.007.

Dardenne, Laurent, Enrico Fraccari, Alessandro Maggioni, Luca Molinaroli, Luca Proserpio, and Eric Winandy. 2015. "Semi-Empirical Modelling of a Variable Speed Scroll Compressor with Vapour Injection." International Journal of Refrigeration 54 (1905): 76–87. https://doi.org/10.1016/j.ijrefrig.2015.03.004.

Dechesne, Bertrand J., Fernando M. Tello-Oquendo, Samuel Gendebien, and Vincent Lemort. 2019. "Residential Air-

Source Heat Pump with Refrigerant Injection and Variable Speed Compressor: Experimental Investigation and Compressor Modeling." International Journal of Refrigeration 108: 79–90. https://doi.org/10.1016/j.ijrefrig.2019.08.034.

Khan, Amjid, and Craig Bradshaw. 2024a. Development of a Residential Scale, Economized, Compressor Load Stand to Measure Compressor Performance Using Low GWP, Flammable Refrigerants. Springer Nature Switzerland. https://doi.org/10.1007/978-3-031-42663-6_66.

Khan, Amjid, and Craig R. Bradshaw. 2023. "Quantitative Comparison of the Performance of Vapor Compression Cycles with Compressor Vapor or Liquid Injection☆." International Journal of Refrigeration 154 (June): 386–94. https://doi.org/10.1016/j.ijrefrig.2023.07.012.

Khan, Amjid, and Craig R Bradshaw. 2024b. "Development of a Black-Box Compressor Model That Captures Vapor-Injection Compared Against Established Black-Box Models" Center for Integrated Building Systems , Oklahoma State University

Lumpkin, Domenique R., Ammar M. Bahman, and Eckhard A. Groll. 2018. "Two-Phase Injected and Vapor-Injected Compression: Experimental Results and Mapping Correlation for a R-407C Scroll Compressor." International Journal of Refrigeration 86 (February): 449–62. https://doi.org/10.1016/j.ijrefrig.2017.11.009.

Ma, Guo Yuan, and Hui Xia Zhao. 2008. "Experimental Study of a Heat Pump System with Flash-Tank Coupled with Scroll Compressor." Energy and Buildings 40 (5): 697–701. https://doi.org/10.1016/j.enbuild.2007.05.003.

Mohsin Tanveer, M., and Craig R. Bradshaw. 2021. "Performance Evaluation of Low-GWP Refrigerants in 1–100 Ton Scroll Compressors." International Journal of Refrigeration 129 (September): 317–31. https://doi.org/10.1016/j.ijrefrig.2021.05.008.

Qiao, Hongtao, Xing Xu, Vikrant Aute, and Reinhard Radermacher. 2015. "Transient Modeling of a Flash Tank Vapor Injection Heat Pump System - Part II: Simulation Results and Experimental Validation." International Journal of Refrigeration 49 (1): 183–94. https://doi.org/10.1016/j.ijrefrig.2014.06.018.

Sun, Haoran, Haitao Hu, Jingwei Wu, Guoliang Ding, Geping Li, Chengyun Wu, Xuyang Wang, and Zhongyuan Lv. 2018. "Modèle de Calcul Théorique Explicite Pour Les Compresseurs à Spirale à Vitesse Variable Avec Injection de Vapeur." International Journal of Refrigeration 88: 402–12.

Tanveer, M. Mohsin, Craig R. Bradshaw, Xin Ding, and Davide Ziviani. 2022. "Mechanistic Chamber Models: A Review of Geometry, Mass Flow, Valve, and Heat Transfer Sub-Models." IJR

Tello-Oquendo, Fernando M., Emilio Navarro-Peris, Francisco Barceló-Ruescas, and José Gonzálvez-Maciá. 2019. "Semi-Empirical Model of Scroll Compressors and Its Extension to Describe Vapor-Injection Compressors. Model Description and Experimental Validation." International Journal of Refrigeration 106 (October): 308–

Tello-Oquendo, Fernando M., Emilio Navarro-Peris, and José Gonzálvez-Maciá. 2017a. "Nouvelle Méthodologie de Caractérisation Des Compresseurs à Spirale à Injection de Vapeur." International Journal of Refrigeration 74: 526–37. https://doi.org/10.1016/j.ijrefrig.2016.11.019.

Tello-Oquendo et al. 2017b. "Nouvelle Méthodologie de Caractérisation Des Compresseurs à Spirale à Injection de Vapeur." International Journal of Refrigeration 74 (February): 526–37.

Wang, Baolong, Wenxing Shi, Linjun Han, and Xianting Li. 2009. "Optimization of Refrigeration System with Gas-Injected Scroll Compressor." International Journal of Refrigeration 32 (7): 1544–54.

Winandy, Eric, Claudio Saavedra Saavedra O, and Jean Lebrun. 2002. "Experimental Analysis and Simplified Modelling of a Hermetic Scroll Refrigeration Compressor." Applied Thermal Engineering 22 (2): 107–20.

Xu, Xing, Yunho Hwang, and Reinhard Radermacher. 2011. "Refrigerant Injection for Heat Pumping/Air Conditioning Systems: Literature Review and Challenges Discussions." International Journal of Refrigeration 34 (2): 402–15. https://doi.org/10.1016/J.IJREFRIG.2010.09.015.

Yang, Minghong, Baolong Wang, Xianting Li, Wenxing Shi, and Leping Zhang. 2015. "Evaluation of Two-Phase Suction, Liquid Injection and Two-Phase Injection for Decreasing the Discharge Temperature of the R32 Scroll Compressor." International Journal of Refrigeration 59 (November): 269–80. https://doi.org/10.1016/j.ijrefrig.2015.08.004.

ACKNOWLEDGEMENT

The authors would like to acknowledge the Center for Integrated Building Systems, an Industry/University cooperative research center at Oklahoma State University, USA for funding this study.